201970: gold-bearing grains, Hillside gold prospect

(Kelly Group, East Pilbara Terrane)

Sample type	Gold-bearing grains
Specimens	Three specimens comprising six grains
Total weight	0.8 g
Sample location	Hillside gold prospect, about 52 km west-northwest of Nullagine
Coordinates	MGA zone 50, 774900E 7600100N
Datum	GDA94
1:250 000 map sheet	Marble Bar (SF 50-8)
1:100 000 map sheet	Split Rock (2854)
Tenement	E 45/4685
Collector	Macarthur Minerals

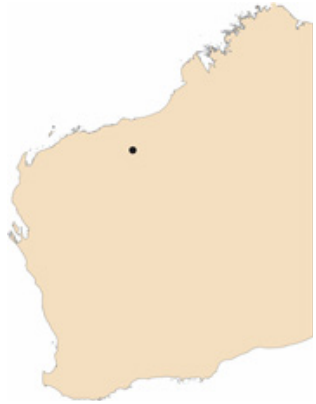

Location and sampling

The sample was provided by Macarthur Minerals in October 2018. It was collected at the Hillside gold prospect in the East Pilbara Terrane. The sample comprises one gold-bearing grain collected from a gossan (specimen A; Fig. 1a), four gold grains from alluvium along a creek that cuts through the gossan (specimen B; Fig. 1b), and one gold-bearing grain from a nearby quartz reef (specimen C, Fig. 1c; Macarthur Minerals, 2018, written comm., 30 October).

Geological context

The Hillside gold prospect is located about 1.4 km west of the Coongan fault system, which is inferred to be a bounding structure to a central graben (Ferguson and Ruddock, 2001). The bedrock comprises massive to locally pyroxene–spinifex-textured, pillowed komatiitic metabasalt of the 3350–3335 Ma Euro Basalt (Hickman, 2021b) of the 3350–3315 Ma Kelly Group (Hickman, 2021c), which is part of the Kelly Large Igneous Province (Hickman, 2021a, 2013; GSWA, 2014).

Several gold prospects (Corboy, Corboy Southeast, Edelweiss, and Stubbs) are located 5–6 km north from the Hillside prospect and about 0.5 – 1.3 km west of the Coongan fault system (Bagas et al, 2004). A grab sample from Corboy assayed 33.7 g/t Au, and drilling at Edelweiss intersected gold–pyrite–chalcopyrite mineralization grading 12.3 g/t Au over 5.2 m. These gold deposits are hosted by a thick sequence of high-Mg metabasalt of the Euro Basalt, and are spatially associated with north-northeasterly striking quartz veins (Ferguson and Ruddock, 2001; Bagas et al, 2004).

The nearest regolith landform is an alluvial–fluvial unit comprising unconsolidated gravel, sand, silt and clay in active, but poorly defined, drainage channels on a floodplain. The present-day drainage locally dissects residual or relict, variably silicified, massive, nodular and cavernous calcrete (GSWA, 2014).

Methodology

The specimens were photographed and weighed, their overall morphology and external features, such as colour, roundness, surface relief, coatings, mineral inclusions and mineral assemblages, were recorded using visual morphometry. The raw surfaces of the samples were analysed using scanning electron microscopy with energy-dispersive X-ray spectroscopy (SEM-EDS). The specimens were mounted in epoxy resin and polished to expose their microstructure and inclusions for examination using reflected-light microscopy and SEM-EDS. Gold microchemistry was determined by laser ablation inductively coupled plasma mass spectrometry (LA-ICP-MS), calibrated against certified gold reference materials (CRM; Murray, 2009). The specimens were ablated in duplicate or triplicate along 0.5 mm-long traverses and average values calculated for elements present in the CRM. Gold surfaces were repolished after laser ablation, etched with aqua regia, and internal structures examined using reflected-light microscopy. Details of these methods are described in Hancock and Beardsmore (2020).

Morphology

Specimen A is a 4 × 3 × 3 mm rock chip (Fig. 1a) and consists of intermingled goethite, quartz and gold. There are large parallel scratches on its external surface.

Specimen B comprises four ferruginous gold–quartz grains (Fig. 1b), which have dimensions 5 × 5 × 4 mm, 5 × 4 × 3 mm, 4 × 3 × 3 mm, and 5 × 2 × 2 mm. The largest grain is well rounded, and the other three are slightly rounded and have irregular shapes with spongy and pitted surfaces.

Specimen C is a gold-bearing piece of white quartz, with dimensions 7 × 4 × 4 mm (Fig. 1c), and is considered to represent primary gold mineralization at the Hillside gold prospect.

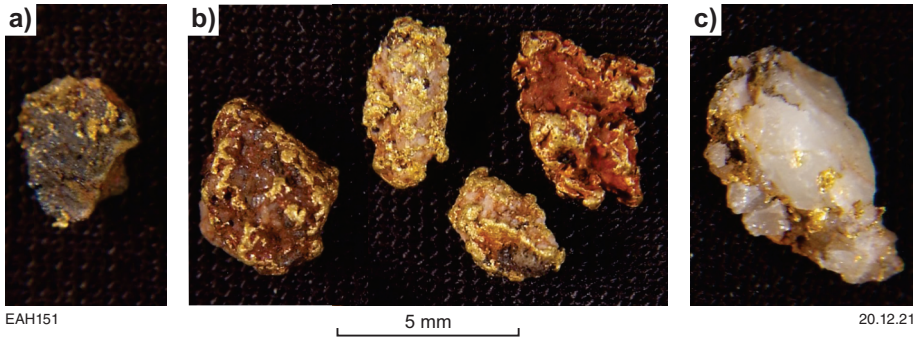

Figure 1. **Six gold grains comprise sample 201970: gold-bearing grains, Hillside gold prospect: a) specimen A; b) specimen B; c) specimen C**

SEM-EDS analysis of raw surfaces

The exposed surface of gold in specimen A contains 3% Ag and shows unaltered, stepped growth features (Fig. 2a). Pits in this surface are filled with kaolinite and Fe–Mg chlorite. Very small plates of gold are disseminated in the clay and on the surface of Fe-oxide minerals.

The surfaces of the three smallest gold grains in specimen B also contain 2–3% Ag, have stepped growth features and pits containing Fe- and K-rich clays, Fe-oxide minerals and K-feldspar inclusions (Fig. 2b). The surface of the most rounded gold grain with large Fe-oxide minerals shows significant damage and no detectable Ag (Fig. 2b).

Specimen C comprises relatively large quartz grains cemented by narrow, irregular veinlets of gold with a stepped and striated surface containing 3% Ag and some Fe-rich illite in pits (Fig. 2c).

Optical microscopy of polished surfaces

Gold in specimen A is disseminated in heterogeneous, zoned, porous, spongy goethite, which also contains isolated quartz grains (Fig. 3a).

The interiors of the grains of specimen B vary from massive, irregular gold to intergrowths of gold with spongy goethite. The largest, most rounded grain is mainly massive gold with dispersed, porous goethite, irregular to euhedral quartz grains, and reduced Ag along micro-veinlets and surrounding dissolution pores within a wide outer rim (Fig. 3b).

Specimen C consists mainly of granular quartz encrusted with gold along grain boundaries (Fig. 3c).

SEM-EDS analysis of polished surfaces

Massive gold in specimen A contains 4% Ag, and inclusions of mica flakes and heterogeneous goethite (Fig. 4a). Darker Al-rich and lighter Fe-rich phases are located in goethite around porous dissolution zones, together with small gold particles. Botryoidal goethite crystals fill a cavity in massive goethite.

Gold in the smaller grains comprising specimen B contains 3.5 – 4.0% Ag and very small inclusions of Al-oxide minerals and chlorite. Massive gold in the larger, more rounded grain contains 5.5% Ag, and finely disseminated gold contains 2% Ag. There are also a few small dolomite inclusions in this grain.

Gold in specimen C contains 4% Ag and small inclusions of Fe–Mg chlorite (Fig. 4b).

LA-ICP-MS analysis

Analyses consistently detected Ag, Cu and Hg within the gold grains, in concentrations higher than the instrumental detection limit, and probably occurring as limited solid solutions in the gold. Other trace elements were detected only sporadically in low (sub ppm) concentrations, possibly occurring in micro- and nano-inclusions.

With the exception of the large, rounded grain in specimen B, all gold has low Ag (3–4%), with moderate Cu (500–700 ppm) and Hg (300–900 ppm) (Table 1). The gold in specimen C returned a lower Ag content along two traverses (2.2 and 2.5%) compared with SEM-EDS results (4%), yet shows no evidence of silver-depleted zones. A possible explanation is that insufficient gold sample was analysed along the two traverses.

The rounded grain in specimen B contains significantly higher Ag (4.5 – 6.5%), lower Cu (148–357 ppm) and very high Hg (0.3 – 0.9%).

Lithophile elements detected in gold (Table 2) result from partial ablation of associated regolith materials. There are no calibration standards for these materials and no data have been calculated.

Acid etching

The internal fabrics of massive gold in all specimens are polycrystalline, and exhibit variable degrees of deformation.

Angular gold contained in the goethite matrix of specimen A has a twinned, deformed and partly recrystallized texture with minor granulation (Fig. 5a).

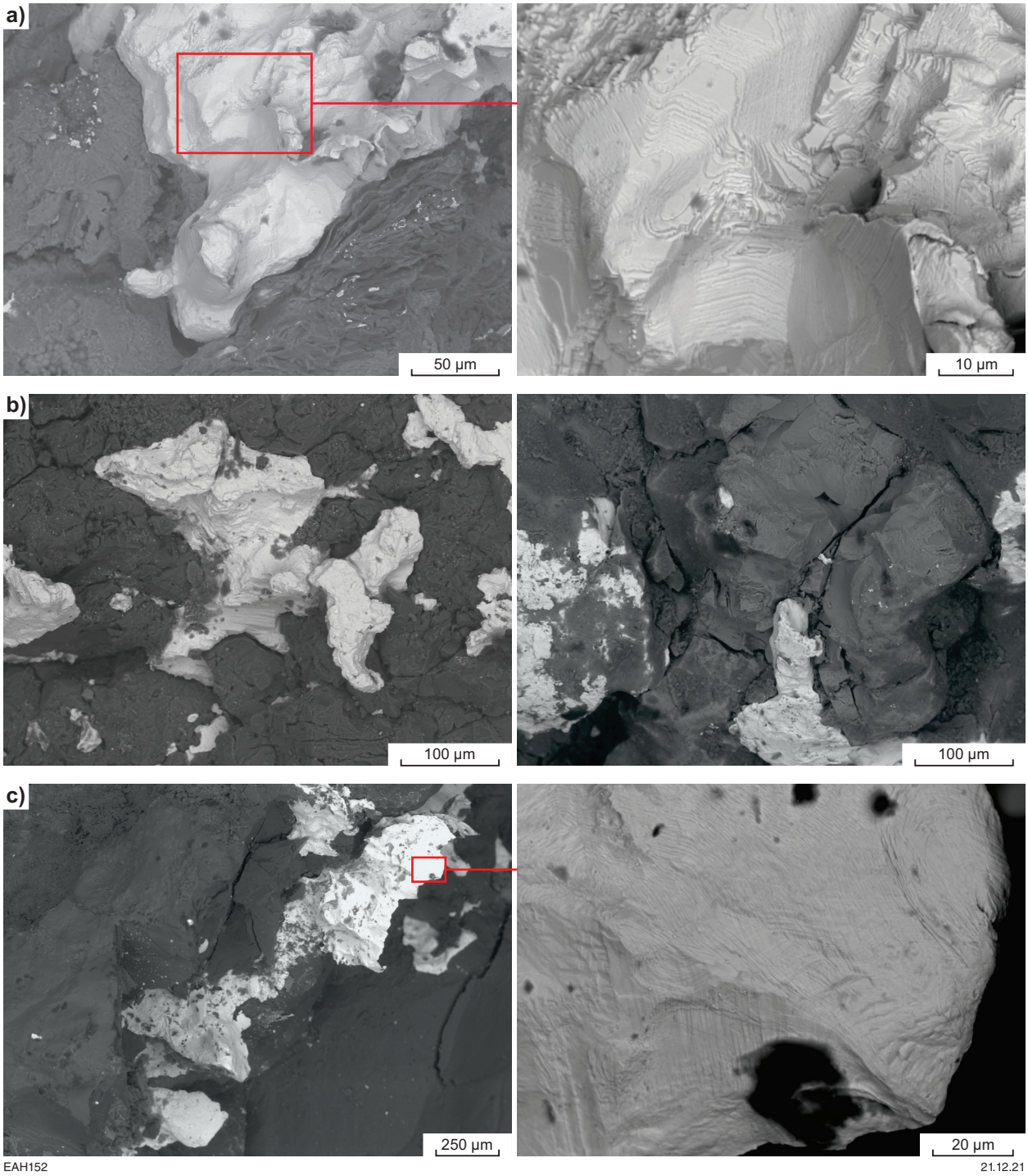

Figure 2. **Backscattered electron (BSE) images of sample 201970: gold-bearing grains, Hillside gold prospect: a) specimen A; b) specimen B; c) specimen C**

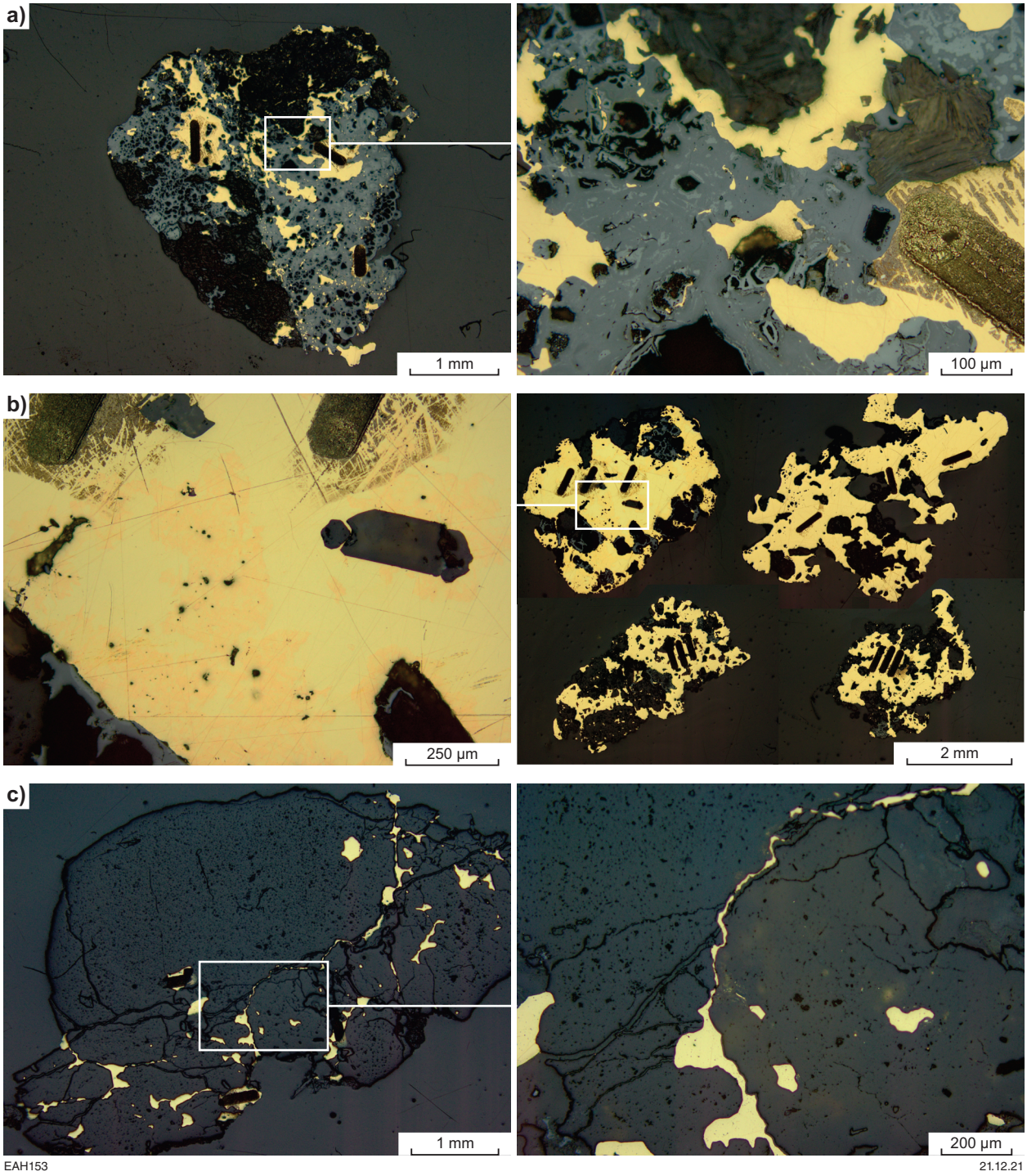

Figure 3. **Reflected-light photomicrographs of cut and polished sample 201970: gold-bearing grains, Hillside gold prospect: a) specimen A; b) specimen B; c) specimen C. Dark elongate lines are laser ablation tracks produced during LA-ICP-MS analyses**

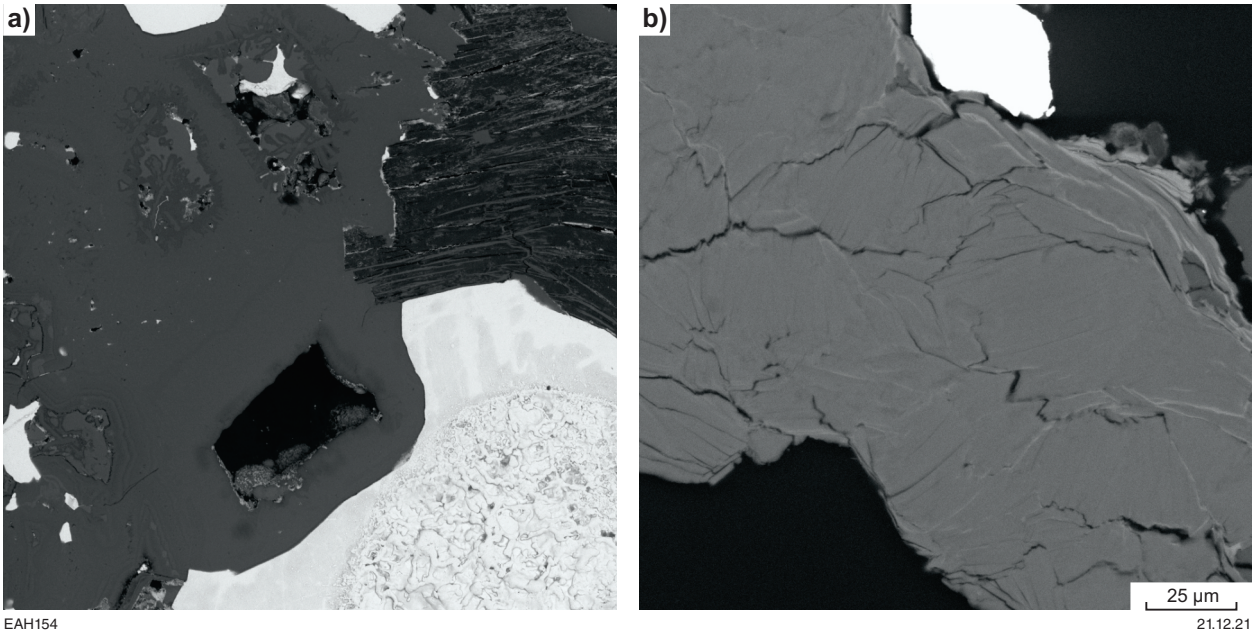

Figure 4. **BSE images of mineral inclusions in cut and polished sample 201970: gold-bearing grains, Hillside gold prospect: a) specimen B; b) specimen C**

Table 1. **LA-ICP-MS data for selected elements in sample 201970: gold-bearing grains, Hillside prospect**

Specimen	*Ag (%)*	*Cu (ppm)*	*Hg (ppm)*	*Minor elements*
A	3.8, 5.0, 5.1	480, 596, 627	569, 881, 1020	Mg
B	3.1, 3.2, 3.2, 3.3, 3.3, 3.5, 3.5, 3.9, 4.3 rounded grain: 4.5, 5.9, 6.5	500-700 rounded grain: 148, 271, 357	300-400 rounded grain: 3675, 8446, 9455	Mg
C	2.2, 2.5, 3.7	404, 470, 578	479, 633, 896	Mg

All gold in specimen B has a polycrystalline, deformed fabric with incoherent twinning and curved micro-grain boundaries (Fig. 5b). Chemical alteration of the internal fabrics is marked by narrow intergranular veinlets and corrosion rims up to 80 µm thick. The original coarsely granular fabric of the rounded grain is extensively damaged, and now resembles a highly deformed melting texture (Fig. 5b).

Gold in specimen C shows simple polysynthetic twinning with only minor deformation (Fig. 5c).

Interpretation

All specimens, with the exception of the large, rounded grain in specimen B, originated from a single ore-bearing solution and have undergone minimal alteration and transportation from their primary source. These grains were most likely derived from the same local source as those comprising sample 201971 (Hancock et al., 2022). Specimen C and specimen B of sample 201971 typify primary gold mineralization in the area.

The different physical and chemical characteristics of the rounded gold grain in specimen B indicate that it most likely originated from a different primary source and was transported into the Hillside area.

Table 2. LA-ICP-MS compositional data for sample 201970: gold-bearing grains, Hillside prospect

Specimen and laser ablation track	Unit	^{7}Li	^{9}Be	^{11}B	^{23}Na	^{25}Mg	^{27}Al	^{29}Si	^{44}Ca	^{45}Sc	^{49}Ti	^{51}V	^{53}Cr	^{55}Mn	^{57}Fe	^{59}Co	^{60}Ni	^{65}Cu
A	cps		2			235	39597			18	9	85		131	473	22	7	73723
A	cps					3489	117		2512		3	4	153	7403	1329	15252	295	77646
A	cps				6082	592	3468		159	11	3	331	33	6835	9342	393	72	59392
C	cps					64	119			5	4		7			1	7	58174
C	cps					136	807	36070	100	280	5		37	1467	2.5	32	2	71568
C	cps		2		4413	1879	15195	52558	637	389	21	1227	3959	64151	1020	1426.275	273	50024
B-1	cps			19		142	466				4	2	18				2	33516
B-1	cps			8		112	1082			7	3		36			5	2	44148
B-1	cps		3	25		447	13612		214	37	18	64	88	88	1368	8	32	18360
B-2	cps	62				48	19682	458	10	2	2	6	42		15	2		63415
B-2	cps			9		145	35596		2711	21	12	23	24	1276	325	9	8	75494
B-2	cps		2	43	27319	107	1971544	48292	737	294	11	61	41	271	581	12	23	65050
B-3	cps					38	302				5		112		2	2	3	75005
B-3	cps		2	51		174	1606				1	29	3671		11	7	6	88647
B-3	cps			53		77	581		19		7	6	32		1810	5	8	81725
B-4	cps	468	2	54	41044	1009	461356	21431	136	107	5	33	3468	9	25	20	50	68181
B-4	cps	2684		183	112397	2233	3722661	173642	2064	787	13	112	9945	270	372	94	560	65627
B-4	cps	2638	5	88	81993	908	3319902	157166	1009	486	15	149	6568	1010	1483	59	202	78357
A	ppm					2.82					0.20						0.07	596
A	ppm					41.78					0.07						2.98	627
A	ppm					7.09					0.05						0.72	480
C	ppm					0.76					0.08						0.07	470
C	ppm					1.63					0.11						0.02	578
C	ppm					22.50					0.46						2.76	404
B-1	ppm					1.70					0.09						0.02	271
B-1	ppm					1.34					0.05						0.02	357
B-1	ppm					5.35					0.38						0.32	148
B-2	ppm					0.57					0.03							512
B-2	ppm					1.73					0.26						0.08	610
B-2	ppm					1.28					0.24						0.23	525
B-3	ppm					0.45					0.11						0.03	606
B-3	ppm					2.08					0.02						0.06	716
B-3	ppm					0.92					0.14						0.08	660
B-4	ppm					12.08					0.11						0.50	551
B-4	ppm					26.74					0.28						5.66	530
B-4	ppm					10.88					0.33						2.04	633

Specimen and laser ablation track	Unit	^{66}Zn	^{69}Ga	^{72}Ge	^{75}As	^{82}Se	^{85}Rb	^{88}Sr	^{89}Y	^{90}Zr	^{93}Nb	^{98}Mo	^{101}Ru	^{103}Rh	^{108}Pd	^{109}Ag	^{111}Cd	^{115}In
A	cps	12	7	2			3	8				2		3	5	10550261	46	4
A	cps	34		5	4763		2	24	3					2	3	10409346	51	
A	cps	37	154	29	45	8	3	149	21	2	4		1	2	3	7772726	29	1
C	cps				6			8	1	3	5			3	5	7570523.94	18	2
C	cps	16	3	1		5		7			3			3	5	5249574.47	29	
C	cps	49	160.04	8	74		3	358.71	117.53	12	4	1		4	3	4617293.235	12	
B-1	cps	8			4			1		2	15	1		2	6	12080402	7	2
B-1	cps	14		2	6			3	3	3	8	3			5	13486373	13	
B-1	cps	34	13	4	5			20	68	4	3			3	15	9345881	6	
B-2	cps	25	3	8		3		6	1		3			2	6	7220049	27	2
B-2	cps	14	3		5	1		159	9	1	9			3	4	8003693	27	4
B-2	cps	28	461	3			1726	205		2					3	6613725	19	2
B-3	cps	15					5	7			2	1			7	6459209	42	3
B-3	cps	18	14	3			8	7			16	1		2	9	7697825	66	
B-3	cps	31			7		2	9	1	5	13			3	8	6714485	46	1
B-4	cps	28	76	8	5		89	52	1	2	11	2		2		7334513	19	2
B-4	cps	119	1815	15			4002	236	13	11	17		2	1	2	6821317	21	
B-4	cps	51	1951	4	12		2974	162	8	4	32			2	5	8764807	36	
A	ppm	0.14												0.006	0.04	51190		0.007
A	ppm	0.39			58.24									0.004	0.02	50506		
A	ppm	0.42			0.54	0.64								0.004	0.02	37713		0.002
C	ppm				0.07									0.006	0.04	36732		0.004
C	ppm	0.18				0.36								0.007	0.03	25471		
C	ppm	0.56			0.90									0.009	0.02	22403		
B-1	ppm	0.09			0.04									0.005	0.04	58614		0.003
B-1	ppm	0.16			0.07										0.03	65436		
B-1	ppm	0.39			0.06									0.006	0.11	45346		
B-2	ppm	0.28				0.24								0.004	0.04	35032		0.003
B-2	ppm	0.16			0.06	0.08								0.007	0.03	38834		0.008
B-2	ppm	0.32													0.02	32090		0.004
B-3	ppm	0.17													0.05	31340		0.006
B-3	ppm	0.21												0.004	0.06	37350		
B-3	ppm	0.35			0.09									0.007	0.06	32579		0.002
B-4	ppm	0.32			0.06									0.005		35587		0.004
B-4	ppm	1.37												0.002	0.01	33097		
B-4	ppm	0.59			0.15									0.004	0.04	42527		

Notes: cps, count per second; ppm, parts per million

Table 2. continued

Specimen and laser ablation track	Unit	^{120}Sn	^{121}Sb	^{126}Te	^{133}Cs	^{138}Ba	^{139}La	^{140}Ce	^{141}Pr	^{145}Nd	^{151}Eu	^{157}Gd	^{159}Tb	^{162}Dy	^{165}Ho	^{167}Er	^{169}Tm	^{172}Yb
A	cps	14		3	5	27		2		3			2					
A	cps	49	7	13	3	3			1					3				
A	cps	16	5	3		731	26	22	13	2	2	2	2	2	2		1	
C	cps	9	5	1		3				1.5		2	2	2			1	
C	cps	11	8	3	2	12		5			2	2			1	1		2
C	cps	17	19	46	2	1240	42	25	22	15	13	9	13	20	15	7	5	9
B-1	cps	17		1	4	2		1								2		
B-1	cps	25		3	2	4	2								1			
B-1	cps	22	3	3	2	19	18	5	8	4	2	6	2	6	3			
B-2	cps	12		9		4		2		2		3					2	1
B-2	cps	15		15	3	16		1		1	1				1			3
B-2	cps	21		8	8	4637	3	2		2		1				2		
B-3	cps	17	2			2		2		2						2		2
B-3	cps	22	9	5		1		1										
B-3	cps	11	5	1	5	2	2	2	2	1			4	1				2
B-4	cps	7	8	9	7	641												2
B-4	cps	24	30	16	19	15717	5	1		1								
B-4	cps	26	18	80	29	10152		1							2			
A	ppm	0.06		0.06														
A	ppm	0.22	0.03	0.24														
A	ppm	0.07	0.02	0.06														
C	ppm	0.04	0.02	0.02														
C	ppm	0.05	0.03	0.05														
C	ppm	0.07	0.07	0.84														
B-1	ppm	0.08		0.02														
B-1	ppm	0.11		0.06														
B-1	ppm	0.10	0.01	0.05														
B-2	ppm	0.05		0.16														
B-2	ppm	0.07		0.28														
B-2	ppm	0.09		0.15														
B-3	ppm	0.07	0.01															
B-3	ppm	0.10	0.04	0.09														
B-3	ppm	0.05	0.02	0.02														
B-4	ppm	0.03	0.03	0.16														
B-4	ppm	0.11	0.11	0.28														
B-4	ppm	0.12	0.07	1.46														

Specimen and laser ablation track	Unit	^{175}Lu	^{178}Hf	^{181}Ta	^{182}W	^{185}Re	^{189}Os	^{193}Ir	^{195}Pt	^{202}Hg	^{205}Tl	^{208}Pb	^{209}Bi	^{232}Th	^{238}U
A	cps									295919		2	13		
A	cps				1	2				255428	1	9	30		1
A	cps	2		2						164945	2	17	24		2
C	cps				1		1		1	259713	2	13			
C	cps	2				1				138932	1		5		
C	cps	7			2			1	1	183501	1	23	23		2
B-1	cps				1	1			1	2449302					
B-1	cps	1						1		2741935	2	1	4		
B-1	cps	4								1065813		12	4		2
B-2	cps									94112			10		
B-2	cps	2	2							103980		8	5	2	
B-2	cps	1	1	2		1		1	1	105181	5	6	10		
B-3	cps		1				1			82960			11		2
B-3	cps		1	2	2	1				106056		12	7		4
B-3	cps						1			91870		25	14	2	4
B-4	cps	2			1					95350	2	15	20	1	1
B-4	cps		1	1	1			1		115433	41	32	24		2
B-4	cps		2							127193			2		
A	ppm									1020		0.01	0.028		
A	ppm									881		0.03	0.063		
A	ppm									569		0.05	0.051		
C	ppm									896		0.04			
C	ppm									479			0.010		
C	ppm									633		0.07	0.049		
B-1	ppm								0.014	8446					
B-1	ppm									9455		0.003	0.009		
B-1	ppm									3675		0.04	0.009		
B-2	ppm									325			0.021		
B-2	ppm									359		0.03	0.011		
B-2	ppm								0.014	363		0.02	0.020		
B-3	ppm									286			0.022		
B-3	ppm									366		0.04	0.015		
B-3	ppm									317		0.08	0.030		
B-4	ppm									329		0.05	0.042		
B-4	ppm									398		0.10	0.050		
B-4	ppm									439			0.004		

Notes: cps, count per second; ppm, parts per million

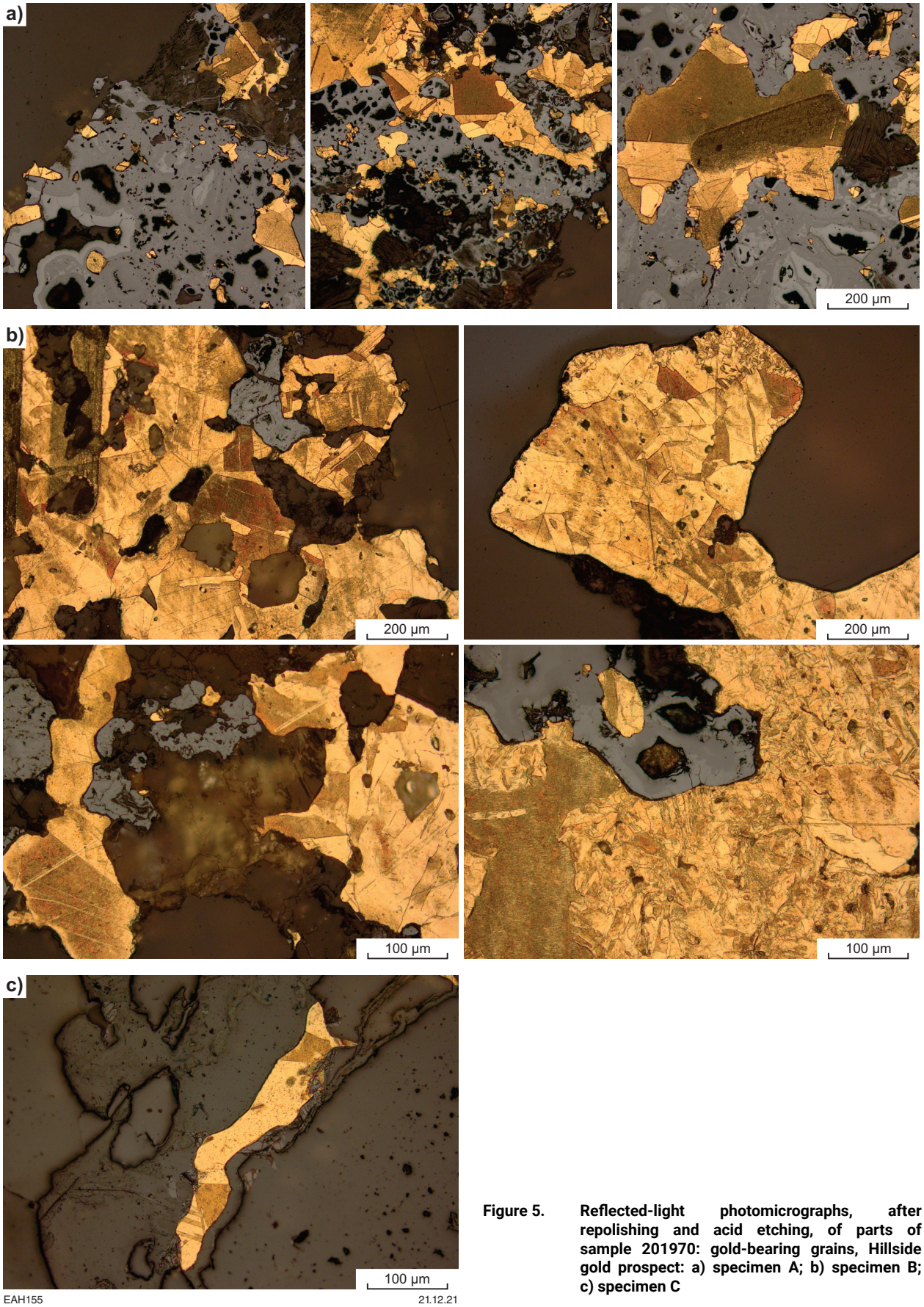

Figure 5. **Reflected-light photomicrographs, after repolishing and acid etching, of parts of sample 201970: gold-bearing grains, Hillside gold prospect: a) specimen A; b) specimen B; c) specimen C**

References

Bagas, L, Van Kranendonk, MJ and Pawley, M 2004, Geology of the Split Rock 1:100 000 sheet: Geological Survey of Western Australia, 1:100 000 Geological Series Explanatory Notes, 43p.

Ferguson, KM and Ruddock, I 2001, Mineral occurrences and exploration potential of the east Pilbara: Geological Survey of Western Australia, Report 81, 114p.

Geological Survey of Western Australia 2014, Pilbara, 2014: Geological Survey of Western Australia, Geological Information Series, data package.

Hancock, EA and Beardsmore, TJ 2020, Provenance fingerprinting of gold from the Kurnalpi Goldfield: Geological Survey of Western Australia, Report 212, 21p.

Hancock, EA, Blay, OA and Beardsmore, TJ 2022, 201971: gold-bearing grains, Hillside gold prospect; GSWA Mineralogy Record 5: Geological Survey of Western Australia, 8p.

Hickman, AH 2013, Split Rock, WA Sheet 2854 (Second Edition): Geological Survey of Western Australia, 1:100 000 Geological Series.

Hickman, AH 2021a, East Pilbara Craton: a record of one billion years in the growth of Archean continental crust: Geological Survey of Western Australia, Report 143, 187p.

Hickman, AH 2021b, Euro Basalt (A-KEe-b): Geological Survey of Western Australia, WA Geology Online, Explanatory Notes extract, viewed 28 March 2022, <www.dmirs.gov.au/ens>.

Hickman, AH 2021c, Kelly Group (A-KE-xb-f): Geological Survey of Western Australia, WA Geology Online, Explanatory Notes extract, viewed 28 March 2022, <www.dmirs.gov.au/ens>.

Murray, S 2009, LBMA certified reference materials. Gold project final update: The London Bullion Market Association, Alchemist, no. 55, p. 11–12.

Recommended reference for this publication

Hancock, EA, Blay, OA and Beardsmore, TJ 2022, 201970: gold-bearing grains, Hillside gold prospect; GSWA Mineralogy Record 4: Geological Survey of Western Australia, 9p.